

# Three-dimensional gyrofluid filament simulations in tokamak scrape-off layers

M. Wiesenberger, M. Held, and A. Kendl

*Institute for Ion Physics and Applied Physics, Universität Innsbruck, 6020 Innsbruck, Austria*

## Introduction

We develop efficient numerical algorithms and full-F gyrofluid models for seeded filament convection in the scrape-off-layer of magnetically confined fusion plasmas. We investigate coordinate systems that are aligned with the magnetic flux surfaces. We successfully implemented a near conformal and an orthogonal grid. The solution of a general elliptic equation, which was discretized with the local discontinuous Galerkin methods, converges with superconvergent order. On the other side, we study a fully nonlinear three-dimensional full-F gyrofluid model in a simple slab magnetic geometry. We include particle source terms to account for losses through the sheath. The literature [1, 2] proposes to also use an effective drag in the velocity equation. However, we show that this term leads to an unpractical energy sink/source in the energy conservation equation. We propose to disregard the drag term in the velocity equation and show that the gyrofluid energy subtracted by a suitable background term is still conserved.

## Grid generation

The general problem is to derive a curvilinear coordinate system  $(x, y)$  that covers the region bounded by two flux surfaces  $\psi(R, Z)$ , where  $(R, Z)$  are cylindrical coordinates. Coordinate lines must align with the magnetic flux surfaces  $\psi$  at least at the boundary. This ensures that field lines do not intersect the boundary of the computational domain, which is advantageous for the computation of parallel derivatives as in Reference [3]. We recover the near conformal grid proposed by Reference [4] with the properties  $\sqrt{g}^{-1} = g^{xx} = f(\psi)^2 (\nabla \psi)^2$  and  $g^{yy} = ((g^{xx})^2 + (g^{xy})^2) / g^{xx}$ . Here,  $f(\psi)$  is a flux-function used to normalize the poloidal coordinate  $y$ . This grid is nearly conformal in the sense that the so-called conformal ratio  $R_c = g^{yy}/g^{xx}$  is close to unity.

On the other hand we can also construct orthogonal coordinates with  $g^{xy} = 0$ ,  $g^{xx} = f^2(\nabla \psi)^2$ ,  $g^{yy} = g^2(\nabla \psi)^2$  and  $\sqrt{g}^{-1} = fg(\nabla \psi)^2$ . We show both grids in Figure 1. As expected the near conformal grid distributes cells more evenly across the domain and exhibits less deformation when compared to the orthogonal grid. However, only the orthogonal grid can easily handle Neumann boundary condition since these define the derivative perpendicular to the boundary.

We define  $\nabla_{\perp} := -\hat{e}_{\varphi} \times \hat{e}_{\varphi} \times \nabla$  and the general elliptic equation (cf. polarisation equation in

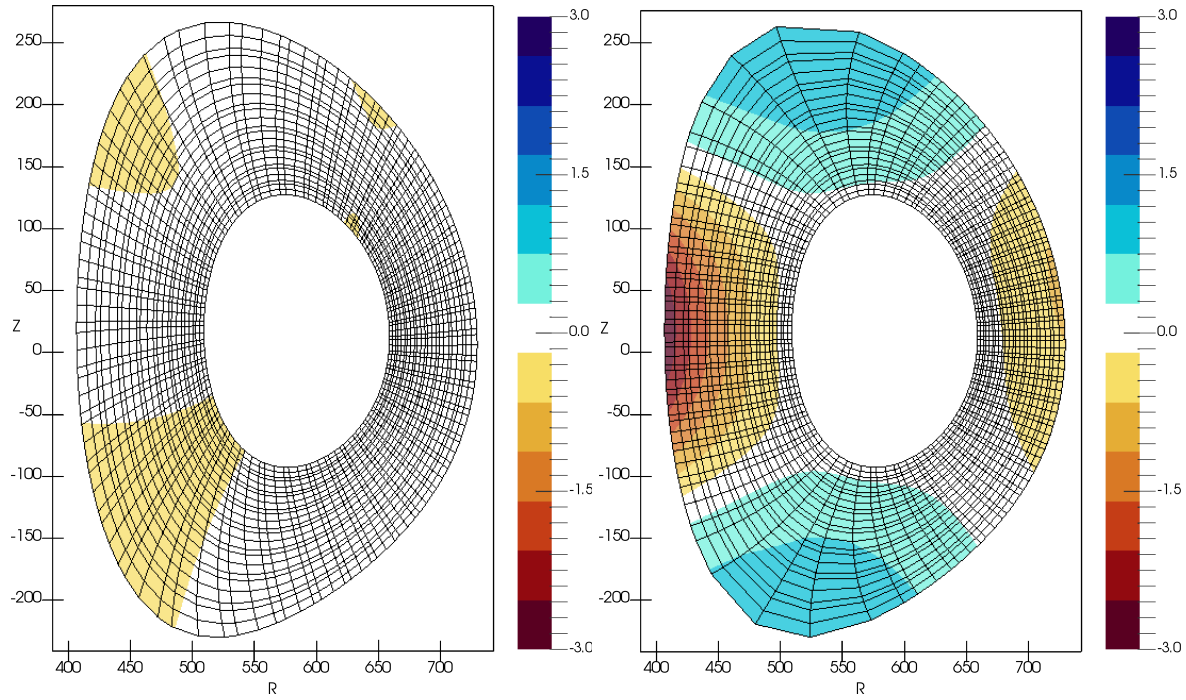


Figure 1: Conformal ratio  $R_c - 1$  for a near conformal grid (left) and orthogonal grid (right) with equal number of grid points  $P = 3, N_x = 8, N_y = 40$ . The conformal grid distributes the cells more evenly across the domain.

the next Section)

$$\nabla \cdot (\chi \nabla_{\perp} f) = \frac{1}{\sqrt{g}} [\partial_x (\sqrt{g} \chi (g^{xx} \partial_x f + g^{xy} \partial_y f)) + \partial_y (\sqrt{g} \chi (g^{yx} \partial_x f + g^{yy} \partial_y f))] = \rho \quad (1)$$

We use this equation to test the quality of our meshes in Table 1 with the help of our library FELTOR ([www.github.com/feltor-dev/feltor](https://www.github.com/feltor-dev/feltor)). We notice that the solution converges with order 4 in the near conformal grid, although only order 3 can be expected from the 2nd order polynomials. In the orthogonal grid the convergence rate deteriorates by 5% for higher resolutions.

| $N_y = 5N_x$ | # iterations | $L^2$ error | order | # iterations | $L^2$ error | order |  |
|--------------|--------------|-------------|-------|--------------|-------------|-------|--|
| conformal    |              |             |       | orthogonal   |             |       |  |
| 40           | 1115         | 1.43E-01    | -     | 1054         | 1.54E-01    | -     |  |
| 80           | 2029         | 8.86E-03    | 4.02  | 2093         | 9.68E-03    | 3.99  |  |
| 160          | 3799         | 5.52E-04    | 4.00  | 3798         | 6.54E-04    | 3.89  |  |
| 320          | 6844         | 3.47E-05    | 3.99  | 6076         | 4.63E-05    | 3.82  |  |
| 640          | 11670        | 2.19E-06    | 3.99  | 10186        | 3.42E-06    | 3.76  |  |

Table 1: Comparison of the near conformal grids.

We attribute this to the high conformal ratio. We note here that convergence stops for both grids as soon as the X-point is included in the domain, which is due to the diverging volume element.

Let us point out here that if the coordinate  $x$  is aligned to  $\psi$  then  $g^{xx} = f^2(\nabla\psi)^2$  always vanishes at the X-point and that therefore simulations in X-point regions should be treated very carefully.

### Model equations in slab geometry

The simplest consistent geometry possible is a slab geometry. We take a Cartesian coordinate system  $(x, y, z)$ , in which the magnetic field takes the form  $\mathbf{B}(x) = B_0(1 + x/R_0)^{-1}\hat{e}_z$  with the major radius  $R_0$  and a reference magnetic field  $B_0$ . We then have  $\hat{\mathbf{b}} = \hat{e}_z$  and vanishing curvature  $\kappa = \hat{\mathbf{b}} \cdot \nabla \hat{\mathbf{b}} = 0$ . Furthermore, we have  $\nabla_{\parallel} f \equiv \hat{\mathbf{b}} \cdot \nabla f = \partial_z f$ . The perpendicular drift velocity reduces to  $\mathbf{v}_{\perp} = \frac{\hat{\mathbf{b}} \times \nabla \phi}{B} + \frac{T}{q} \frac{\hat{\mathbf{b}} \times \nabla \ln B}{B}$  with the electric potential  $\phi$ . The gyrofluid equations for plasma density  $n_e$ , ion gyrocenter density  $N_i$ , electron parallel velocity  $u_e$  and ion parallel gyrocenter velocity  $U_i$  read

$$\partial_t n_e + \nabla \cdot (n_e u_e \hat{\mathbf{b}} + n_e \mathbf{v}_{\perp}^e) = \Lambda_{n_e} + S_n, \quad (2a)$$

$$\partial_t N_i + \nabla \cdot (N_i U_i \hat{\mathbf{b}} + N_i \mathbf{v}_{\perp}^i) = \Lambda_{N_i} + S_n, \quad (2b)$$

$$m_e n_e (\partial_t u_e + u_e \nabla_{\parallel} u_e + \mathbf{v}_{\perp}^e \cdot \nabla u_e) = -T_e \nabla_{\parallel} n_e + e n_e \nabla_{\parallel} \phi - e n_{e,0} \eta_{\parallel} J_{\parallel} + n_e \Lambda_{u_e}, \quad (2c)$$

$$m_i N_i (\partial_t U_i + U_i \nabla_{\parallel} U_i + \mathbf{v}_{\perp}^i \cdot \nabla U_i) = -T_i \nabla_{\parallel} N_i - e N_i \nabla_{\parallel} \psi + e n_{e,0} \eta_{\parallel} J_{\parallel} + N_i \Lambda_{U_i}, \quad (2d)$$

with the reference density  $n_{e,0}$ , the parallel current  $J_{\parallel} = e(N_i U_i - n_e u_e)$  and the Spitzer resistivity  $\eta_{\parallel} = \frac{\pi e^2 \sqrt{m_e}}{(4\pi\epsilon_0)^2 T_e^{3/2}} \ln \lambda$ . Equations (2) are closed with the polarisation equation

$$n_e = \Gamma_i N_i + \nabla \cdot \left( \frac{N_i}{B^2} \nabla_{\perp} \phi \right). \quad (3)$$

The  $\Lambda$  terms contain (perpendicular) diffusive terms included for numerical stability, while the source term  $S_n$  makes up for losses in the parallel direction through the sheath. Note that we not include the effective drag term  $-(U/N) S_n$  [1, 2] in the velocity equations. This term does not lead to a consistent energy theorem as discussed in the next section.

At the magnetic pre sheath entrance (*se*) we choose the following boundary conditions:

$$U_i^{se} = \pm c_{si}, \quad u_e^{se} = \pm c_{si} \exp(-e\phi/T_e) \quad (4)$$

with  $c_{si} = \sqrt{(T_e + T_i)/m_i} = c_s \sqrt{1 + \tau}$  and  $\tau = T_i/T_e$ . The boundary condition for  $\phi$ ,  $n_e$  and  $N_i$  remain unspecified [2]. At the perpendicular boundaries we choose Dirichlet boundaries for  $N$ ,  $U$  and  $\phi$ , i.e.  $N_e = N_i = N_{eq}$ ,  $U_e = U_i = U_{eq}$ , and  $\phi = \psi = \phi_{eq}$

### Source terms and energy theorem

The background equilibrium fields are chosen such that  $n_e^{eq} = N_i^{eq} = N_{eq}$ ,  $u_e = U_i = U_{eq}$ , and  $\phi_{eq} = \psi_{eq}$ , which results in  $J_{\parallel}^{eq} = 0$ . The equilibrium fields have to fulfill the force balance.

If we assume the time derivative of the equilibrium fields to vanish we immediately get  $\nabla \cdot (\hat{\mathbf{b}}(NU)_{eq}) = S_n$  and  $\nabla_{\parallel} (\frac{1}{2}m_e U_{eq}^2 + T_e \ln N_{eq}) = e \nabla_{\parallel} \phi$ . Enforcing force balance leads to

$$\nabla_{\parallel} \left( \frac{1}{2}(m_e + m_i) U_{eq}^2 + (T_e + T_i) \ln N_{eq} \right) = 0, \quad (5)$$

which is different from [2] due to the effective drag term. The energy theorem is derived by adding  $[T(1 + \ln N) + q\psi + \frac{1}{2}mU^2] \partial_t N$  and  $m(NU - (NU)_{eq}) \partial_t U$ . Integration over the whole volume and assuming boundary terms originating from the  $\partial_t \psi$  terms to vanish (which is true if either  $\phi$  or  $\nabla \phi$  vanishes at the perpendicular boundary) yields

$$\begin{aligned} \partial_t \int_V d^3x \left[ \frac{1}{2}m_i N_i \left( \frac{\nabla_{\perp} \phi}{B} \right)^2 + \sum_s \left( TN \ln N + \frac{1}{2}m(NU - (NU)_{eq}) U \right) \right] \\ \sum_s \int d\mathbf{A} \cdot \hat{\mathbf{b}} \left[ (NU - (NU)_{eq}) \left( T(1 + \ln N) + q\psi + \frac{1}{2}mU^2 \right) \right] = \\ \sum_s \int_V d^3x \left[ \left( T(1 + \ln N) + q\psi + \frac{1}{2}mU^2 \right) \Lambda_N + (NU - (NU)_{eq}) \left( \Lambda_U + \frac{qn_{e,0}\eta_{\parallel} J_{\parallel}}{N} \right) \right], \end{aligned} \quad (6)$$

where we sum over the species  $s \in e, i$ . Here, we have neglected the small term

$-\int_V d^3x m(NU)_{eq} U \nabla \cdot \left( \frac{\hat{\mathbf{b}} \times \nabla \phi}{B} \right)$ . Note that a velocity source term  $S_U$  would appear in (6) on the same footing as  $\Lambda_U$ . However, a conserved energy can only be derived if  $S_U$  can be written in the form  $S_U = \nabla_{\parallel} f$  with an arbitrary function  $f$ .

## Outlook

In the future we want to simulate seeded filaments in the slab geometry and investigate the influence of the parallel resistivity on the transport properties. Further research aims to clarify the influence of finite Larmor radius effects and the nonlinear polarization equation in three-dimensional models as was already done for two-dimensional models [5, 6].

## Acknowledgement

This work was supported by the Austrian Science Fund (FWF) Y398.

## References

- [1] P. C. Stangeby, Plasma Physics Series (IOP Publishing Ltd) (2000)
- [2] L. Easy, F. Militello, J. Omotani, B. Dudson, E. Havlickova, P. Tamain, V. Naulin and A.H. Nielsen, Phys. Plasmas **21** 122515 (2014)
- [3] M. Held, M. Wiesenberger and A. Stegmeir, Comput. Phys. Commun. **199**, 29-39 (2016)
- [4] T. T. Ribeiro and B. D. Scott, IEEE Transactions on Plasma Science **38** 2159-2168 (2010)
- [5] M. Wiesenberger, J. Madsen and A. Kendl, Phys. Plasmas **21** 092301 (2014)
- [6] M. Held, M. Wiesenberger, J. Madsen and A. Kendl, Submitted To: Nucl. Fusion (2016)